

# Tensor Voting Extraction of Vessel Centerlines from Cerebral Angiograms

Yu Ding<sup>1</sup>, Mircea Nicolescu<sup>2</sup>, Dan Farmer<sup>2</sup>, Yao Wang<sup>1</sup>, George Bebis<sup>2</sup>, Fabien Scalzo<sup>1</sup>

<sup>1</sup> Department of Neurology, University of California, Los Angeles (UCLA)

<sup>2</sup> Department of Computer Science, University of Nevada, Reno (UNR)

**Abstract.** The extraction of vessel centerlines from cerebral angiograms is a prerequisite for 2D-3D reconstruction and computational fluid dynamic (CFD) simulations. Many researchers have studied vessel segmentation and centerline extraction on retinal images while less attention and efforts have been devoted to cerebral angiography images. Since cerebral angiograms consist of vessels that are much noisier because of the possible patient movement, it is often a more challenging task compared to working on retinal images. In this study, we propose a multi-scale tensor voting framework to extract the vessel centerlines from cerebral angiograms. The developed framework is evaluated on a dataset of routinely acquired angiograms and reach an accuracy of  $91.75\% \pm 5.07\%$  during our experiments.

## 1 Introduction

Angiography or the imaging of the brain vasculature with X-ray is essential to the diagnosis and treatment of several neurovascular diseases. It provides a fast and accurate way to visualize blood vessels inside the brain. During an angiogram, X-ray images are obtained after injecting contrast dye inside a carotid artery. Although angiography is generally acquired in a 2D biplane mode, it is a useful diagnostic tool, mainly used by neurologists to find clots inside the blood vessels, stenosis, and aneurysms. It is generally combined with a background subtraction operation which reduces the artifacts created by the bones; such an imaging procedure is referred to as Digital Subtraction Angiography (DSA). Blood vessel segmentation is important for many clinical diagnostic tasks such as aneurysms, arteriosclerosis, arteriovenous malformations, vasculitis and tears in the lining of an artery. For some of these diagnostic tasks it is necessary to measure the vessel diameter, length, abnormal branching or bulging of the vessels.

Recently, several research efforts have focused on the study of hemodynamics of blood vessels in the brain using angiograms. For example, perfusion angiography [1] can be used to estimate the blood flow within major arteries of the brain. Other studies have investigated the 2D-3D reconstruction of the vessel for computational fluid dynamic simulations (CFD) [2]. Such simulations and analyses of blood flow are promising to establish imaging markers that are associated with

outcome. Such information can play a major role in the personalization of treatment for several neurovascular diseases. However, the automatic extraction and quantification of blood vessel from angiograms in the brain is particularly challenging and beyond current methods. Manual vessel detection requires trained professionals and it becomes a tedious and reader dependent task when faced with a large number of X-ray images. For that reason, it is important to have an automatic blood vessel detection system. Automating blood vessel segmentation is itself a difficult task due to non-uniform illumination in the images and significant differences in the width of arteries and veins that often lead to an imprecise representation of the vasculature tree.

Several research studies have been done about vessel detection from angiograms while little work has been done on centerline extraction. In 1998, Frangi [3] proposed a multi-scale vessel enhancement filter and it is still in use in many studies nowadays. Staal [4] proposed a ridge-based vessel segmentation method that could reach an accuracy of 0.944 versus 0.947 for a second observer. Hooshyar [5] claimed his method of fuzzy ant colony algorithm could reach an accuracy of 0.933 versus 0.947 for a second observer. Sanjani [6] has combined different approaches before to examine the effect in 2013. Recently, a PSO-algorithm-based method was proposed by Sreejini [7]. In 2016, Christodoulidis implemented small retina segmentation using multi-scale tensor voting. It is worth noting that DSA images of brain vessels (considered in our study) may have much more noise because of the patients movement. In addition, the width of vessels in cerebral DSA images could change on a very large scale while retina vessels change little. Consequently, it is much harder to extract vessels or centerlines from DSA images of brains. In Egger’s work [8], an efficient way to extract catheter centerlines was introduced. Sofka [9] presented an approach of retina vessel centerline in his work. Meanwhile, Yan Xu [10] and Puentes [11] have worked on coronary vessels.

Our work aims at extracting the centerlines of the vessels and remove the noise at the same time. Since tensor voting performs well on curve connection and noise removal [12–14], we adopt a multi-scale approach [15]. As for applying tensor voting on vessel centerlines, Risser [16] has used tensor voting in 3D. Leng [17] has proposed a rapid 2D centerline extraction method based on tensor voting, however, he did not focus on noise removal and his method is designed for retinal images. Compared with previous studies, this paper will present a multi-scale tensor voting framework extracting centerlines from cerebral angiograms based on the idea that vessels have a higher structure consistency than noise.

## 2 Methods

The diagram in Fig.1 shows the pipeline of centerlines extraction from angiograms. We first implement a multi-scale filter on the raw image to capture vessels of different width. Then we extract the skeletons of vessels as well as noise. Next, in order to remove the noise and preserve the small vessels at the same time, a multiscale tensor voting framework is implemented since tensor

voting has a great performance on curve connecting and noise removal [18]. The image is divided into segments and segments with low saliencies during scale changing are removed. After noise removal, the vessels are connected according to the saliency map.

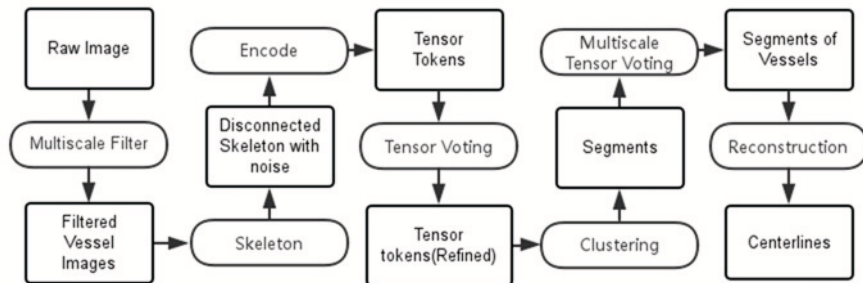


Fig. 1: Overall pipeline of our approach which involves image filtering, skeletonization, tensor voting, clustering and reconstruction.

## 2.1 Dataset

The dataset used to evaluate our framework originates from 19 patients treated at a University Medical Center for acute ischemic stroke. Source images were acquired using 2D DSA. Each run consists of a sequence of 20 frames. The orthogonal angiograms were acquired in an interleaved fashion; one frontal, one sagittal, and so on. The DSA scanning was performed on a Philips Allura Xper FD20<sup>®</sup> Biplane using a routine timed contrast-bolus passage technique. A manual injection of omnipaque 300 was performed at a dilution of 70% (30% saline) such that 10cc of contrast was administered intravenously at an approximate rate of  $5\text{cm}^3/\text{s}$ . The median peak voltage output is 95 Kv. Image sizes were all  $1024 \times 1024$  pixels but were acquired with a different field of view.

## 2.2 Pre-processing

**Multiscale Vessel Enhancement Filter** We applied a multiscale vessel enhancement filter proposed by Frangi [3] to our raw images (Fig. 2) to delineate the vessels. Large scale filtering could remove most of the noise, however, it also filters out the small vessels while smaller scales accentuate the details and the noise at the same time. To account for this problem, we use a multi-scale approach and combine scales from 1 to 15 to allow for details to be preserved. We then select the maximum of these 15 scales for each pixel and set a threshold

proportional to the one obtained by Otsu’s method [19], to preserve as many details as possible. A binary image of the vessel image was extracted as shown in Fig.2.

**Skeleton Extraction** The binary image generated on the previous step was then processed with a skeleton extraction algorithm [20]. Because of the changing width of the main vessels and the existence of junctions, there are some additional branches in areas where vessel width changes and junctions are present. To remove these unwanted branches, we implement a high scale filter to the raw images to detect the main vessels where these unwanted branches always appear (Fig.2).

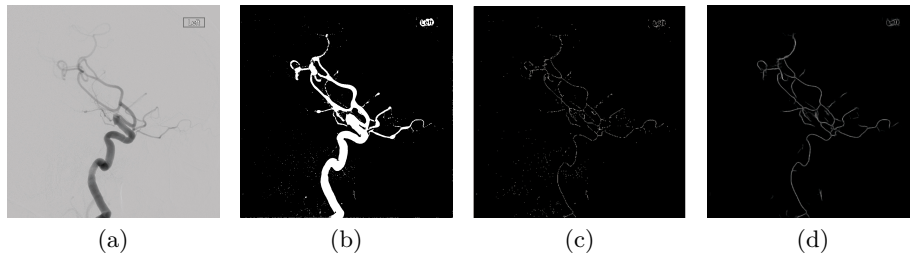


Fig. 2: The steps of our approach. (a) The raw image. (b) After applying the multi-scale filter on the raw image. (c) The skeleton extracted from the filtered image. (d) The saliency map generated after multi-scale tensor voting framework, which could be used to reconnect the vessels.

### 2.3 Multiscale Tensor Voting Framework

Following the pre-processing step, a multi-scale tensor voting framework was implemented in order to remove the noise and connect small vessels. This method works by having structurally salient features enforce each other in a neighborhood, while removing noise and preserving the details extracted in the previous step.

**Tensor Voting Framework** In the tensor voting framework proposed by Medioni [21], each input token is encoded as a second order symmetric tensor to store its information according to the expression below:

$$T = \begin{pmatrix} a_{11} & a_{12} \\ a_{21} & a_{22} \end{pmatrix} = \lambda_1 \mathbf{e}_1 \mathbf{e}_1^T + \lambda_2 \mathbf{e}_2 \mathbf{e}_2^T. \quad (1)$$

where  $\lambda_1$  and  $\lambda_2$  are its eigenvalues and  $\mathbf{e}_1$  and  $\mathbf{e}_2$  are the corresponding eigenvectors, where  $\lambda_1 \geq \lambda_2 \geq 0$ . The tensor can also be decomposed into the form representing its stick and ball components:

$$T = (\lambda_1 - \lambda_2)\mathbf{e}_1\mathbf{e}_1^T + \lambda_2(\mathbf{e}_1\mathbf{e}_1^T + \mathbf{e}_2\mathbf{e}_2^T). \quad (2)$$

These two components represent two types of features: curves and points.  $(\lambda_1 - \lambda_2)$  is the saliency of a curve feature while  $\mathbf{e}_1$  represents the normal curve orientation. Meanwhile,  $\lambda_2$  is the saliency of a point feature. In addition, junction points usually have higher saliencies than noisy points, manifesting higher values of  $\lambda_2$ . Consequently, the saliency of the curves and the points represent the probabilities of local curves or sparse points, deciding the local pattern of the image. In the voting process, each token casts votes to the tokens in its neighborhood, where the neighborhood size is controlled by a scale parameter  $\sigma$  set manually. Here we adopted a closed-form solution to tensor voting proposed by Wu [22]. Suppose we have two tokens  $x_j$  and  $x_i$ , where  $x_j$  is the voter and  $x_i$  is the vote receiver.  $r_{ij}$  is a unit vector pointing from token  $x_j$  to  $x_i$ . The tensor vote at  $x_i$  indicated by  $T_j$  located at  $x_j$  is given by the following expression:

$$S_{ij} = c_{ij}R_{ij}T_jR'_{ij}. \quad (3)$$

where  $c_{ij} = \exp(-\frac{\|x_i - x_j\|^2}{\sigma})$ ,  $R_{ij} = I - 2r_{ij}r_{ij}^T$ ,  $R'_{ij} = (I - \frac{1}{2}r_{ij}r_{ij}^T)R_{ij}$  and  $I$  is an identity. And a structure-aware tensor  $T_i$  can be assigned at each site  $x_i$  by summing up all the  $S_{ij}$  casted by  $x_j$  under the chosen scale  $\sigma$ :

$$T_i = \sum_j S_{ij}. \quad (4)$$

This tensor sum at token  $x_i$  indicates the potential local feature of the token according to the saliencies of its two components as explained above. Here we set  $T_j$  as an identity tensor before voting, assuming every input token has no prior orientation information.

**Grouping and multi-scale tensor voting** The skeleton we extracted after using the multi-scale filter consists of much noise and disconnected vessels. Since noise and small vessels are quite similar while small vessels have higher consistencies in their local structure, it is hard to set a single scale that could filter out noise without losing details. Considering the differences in sizes of vessels, here we adopt a multi-scale way to remove the noise and connect the vessels using tensor voting [23].

The only free parameter of tensor voting framework is  $\sigma$ , which controls the voting scale. When  $\sigma$  is small, it preserves the local structures and details. As  $\sigma$  grows, the results tend to retain only the global configurations, curves becoming smooth. Since we have both main vessels and small ones in our image and they adapt to different scales, we change the scale from a small value to a large one to fit all the vessels. As for noise, it is quite similar to small vessels, however it does not have a high consistency on local structures, so the saliency will decrease sharply compared to small vessels. Consequently, it is feasible to apply the multi-scale framework.

We first implement the single-scale tensor voting framework on the images after pre-processing. Then we segment the vessels into fragments according to the positions, curvatures and the  $\mathbf{e}_1$  of the tokens. The number of segments should be selected carefully since it influences both the processing time and the accuracy of the results. Since we have noise and small vessels that are fragments themselves, how meticulous we segment the main vessels matters the results. In our experiments we found that Large segments tend to losing details for the reason that they always have high saliencies. And small cuts may lose tokens near junctions because the saliencies near junctions would decrease. In practice, we apply large segment first and then small cuts in order to achieve a satisfying outcome.

After segmenting the vessels, we implement an iterative procedure of tensor voting: we change the scale from a small value to a large one and count how many times the saliency of each segment exceeds a certain threshold  $T_s$ . After every iteration, we remove the segments that have a low count of exceeding  $T_s$  and slightly increase the value of  $T_s$ . Since the saliency of segments would increase after removing the noise, a higher value of  $T_s$  is required after each iteration. After the multiscale tensor voting, we reconnect the vessels using the saliency map [24]. Fig.2 shows the saliency map after implementing the framework.

### 3 Experiments

Our experiments test whether the proposed multi-scale tensor voting framework could extract vascular centerlines from DSA images. For our experiments, we used 19 DSA images as input, and compared the results with the ground truth which was established manually by a neurologist. The filter scales range from 1 to 15 to capture as many vessels as possible. Then we extract the skeletons and refine them by the method illustrated above. Next, we input every pixel on the skeletons as a ball tensor into the single scale tensor voting framework. The skeletons are then segmented according to the coordinate, curvature and  $\mathbf{e}_1$  of the tokens. We implement the multi-scale tensor voting on these segments. Since both the scale and the number of segments influence the results, here we adopt a large scale range and a small segment number first for the purpose of removing most noise, and then use a small range and a more meticulous segmentation to erase little noise left near vessels. The two scale ranges we used in our experiments are 20 and 50, focusing on the local characteristics and general structures.

### 4 Results

The results of our experiments are shown in Fig.3, and were evaluated by estimating the sensitivity (true positive rates) and specificity (true negative rates). We follow the formula below:

$$TPR = TP/P. \quad (5)$$

$$TNR = TN/N. \quad (6)$$

$$ACCURACY = (TP + TN)/(P + N). \quad (7)$$

where TPR and TNR are true positive rate and true negative rate respectively, also called sensitivity and specificity, TP, P, TN and N represent true positive, positive, true negative and negative respectively.

We select vessels in the ground truth as true and vessels that in fig.2(d) but not in the ground truth as false. Comparing our results with the ground truth, we select the vessels and the mis-selected vessels in our results as our true positive and false positive respectively. Then we select the vessels that are erased from step 3 to step 42 and compare them with the ground truth. Consequently, the true negative should be the vessels that are erased and absent in the ground truth image while the false negative should be the ones erased but appear in the ground truth. Then we count the total pixels of the vessels we selected by hand as the value of symbols they represent. As a result, we obtain an average sensitivity of  $96.89\% \pm 1.91\%$  and an average specificity of  $82.19\% \pm 6.99\%$ . Besides, our average accuracy was  $91.75\% \pm 5.07\%$ . For other works on retina images, they usually have a specificity of around  $96.89\%$  and a much lower sensitivity. For example, Christodoulidis has reached a sensitivity of  $85.06\%$  and a specificity of  $95.82\%$  [25]. The reason we have a high sensitivity is that we set the parameters empirically to avoid losing details. Moreover, the specificity is affected by the presence of scattered noise in some images.

In Fig.3a and Fig.3b, images contain lower level of noise than those in Fig.3c and Fig.3d. First column is consisted of raw images from 4 patients. In the third column of Fig.3, we show the results and annotate the true negatives in black, the false positives in yellow and the false negatives in red. Ground truth images are shown in the right column. In addition, we overlapped the detection on the raw images to better illustrate the results in the second column. The positive samples and negative samples are selected from the skeleton extracted after filtering: we take the tokens that should be a part of the vessels as positive samples and take the rest of them as negative ones. Sample labeling was conducted manually. Consequently, the accuracy reaches a relatively high value. However, there are some details that are lost from filtering the raw image, even though we set the scale from 1 to 15.

## 5 Conclusion and Future Work

We proposed a multi-scale tensor voting framework for the extraction of vessel centerlines. Although small vessels tend to be fragmented, our method extracts centerlines from noisy DSA images by applying a multi-scale procedure to filter out the noise and preserve as much detail as possible. It can be seen that our framework produced encouraging results as shown in Fig.3. For noisy images, we could remove most sparse noise while the noise with certain structure such as

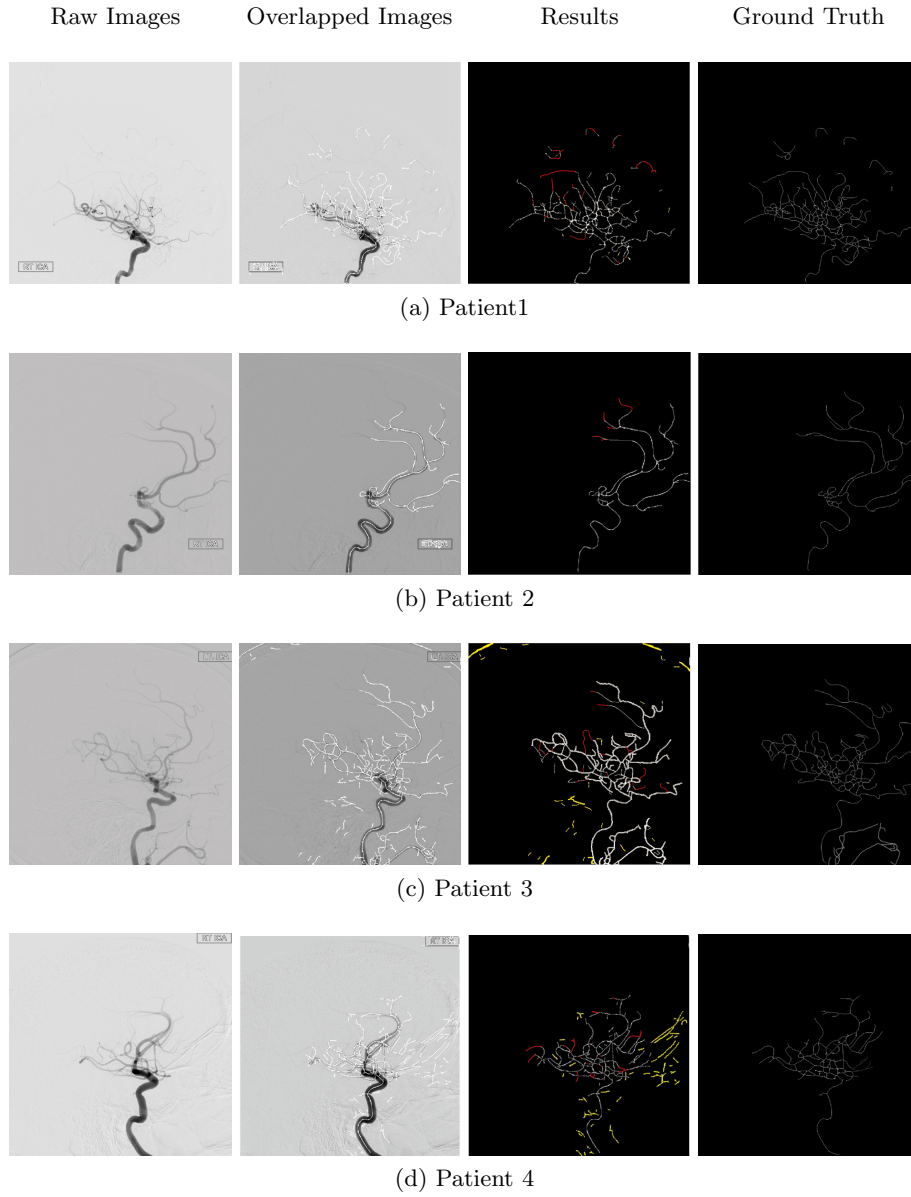


Fig. 3: From left to right: raw images, raw images overlapped with centerlines, our results, ground truth. Results are annotated in the third column (black for true positive, yellow for false positive and red for false negative). Figures from the same row belong to a same patient. The first two rows are images with less noise while the last two rows are ones with much noise. The accuracy of four group of images (from top to bottom): 98.50%, 98.35%, 94.14% and 83.68%

the shadow of skulls still remain. The reason why our method does not perform well on the last two patients (Fig.3c and Fig. 3d) is that they all have noise consisting of long curves due to patient movement. These shadows of skulls have a higher consistency of structure than small vessels, so setting a high threshold to remove them will remove most of the vessels as well.

Other methods that process retinal images usually have an overall accuracy of around 95% with sensitivity under 80% and specificity above 95%. In our results, we have an accuracy of 91.75%, a higher sensitivity of 96.89% and a lower specificity of 82.19%. In addition to being evaluated on a different dataset, our method focuses on noise removal. In our results, we concluded that our multi-scale tensor voting framework performs encouragingly on most cases, however it tends to fail when the noise has a structure similar to vessels. Note that this type of noise could be removed by using a co-registration method between the successive frames of the angiography prior to computing DSA.

## Acknowledgments

Prof. Scalzo was partially supported by a AHA grant 16BGIA27760152, a Spitzer grant, and received hardware donations from Gigabyte, Nvidia, and Intel.

## References

1. Scalzo, F., Liebeskind, D.S.: Perfusion angiography in acute ischemic stroke. *Computational and Mathematical Methods in Medicine* (2016)
2. Scalzo, F., Hao, Q., Walczak, A.M., Hu, X., Hoi, Y., Hoffmann, K.R., Liebeskind, D.S.: Computational hemodynamics in intracranial vessels reconstructed from biplane angiograms. In: *ISVC*. (2010) 359–367
3. Frangi, A.F., Niessen, W.J., Vincken, K.L., Viergever, M.A.: Multiscale vessel enhancement filtering. In: *MICAI*, Springer (1998) 130–137
4. Staal, J., Abràmoff, M.D., Niemeijer, M., Viergever, M.A., van Ginneken, B.: Ridge-based vessel segmentation in color images of the retina. *IEEE transactions on medical imaging* **23** (2004) 501–509
5. Hooshyar, S., Khayati, R.: Retina vessel detection using fuzzy ant colony algorithm. In: *CRV*. (2010) 239–244
6. Sanjani, S.S., Boin, J.B., Bergen, K.: Blood vessel segmentation in retinal fundus images (2013)
7. Sreejini, K., Govindan, V.: Improved multiscale matched filter for retina vessel segmentation using pso algorithm. *Egypt Inform J* **16** (2015) 253–260
8. Egger, J., Mostarkic, Z., Großkopf, S., Freisleben, B.: A fast vessel centerline extraction algorithm for catheter simulation. In: *CBMS*. (2007) 177–182
9. Sofka, M., Stewart, C.V.: Retinal vessel centerline extraction using multiscale matched filters, confidence and edge measures. *IEEE transactions on medical imaging* **25** (2006) 1531–1546
10. Xu, Y., Zhang, H., Li, H., Hu, G.: An improved algorithm for vessel centerline tracking in coronary angiograms. *Computer methods and programs in biomedicine* **88** (2007) 131–143

11. Puentes, J., Roux, C., Garreau, M., Coatrieux, J.L.: Dynamic feature extraction of coronary artery motion using dsa image sequences. *IEEE transactions on medical imaging* **17** (1998) 857–871
12. Tang, C.K., Medioni, G.: Curvature-augmented tensor voting for shape inference from noisy 3d data. *IEEE Trans Pattern Anal Mach Intell* **24** (2002) 858–864
13. Jia, J., Tang, C.K.: Inference of segmented color and texture description by tensor voting. *IEEE Trans Pattern Anal Mach Intell* **26** (2004) 771–786
14. Jia, J., Tang, C.K.: Image repairing: Robust image synthesis by adaptive nd tensor voting. In: *CVPR*. Volume 1. (2003) I–643
15. Loss, L.A., Bebis, G., Parvin, B.: Iterative tensor voting for perceptual grouping of ill-defined curvilinear structures. *IEEE Trans Med Imaging* **30** (2011) 1503–1513
16. Risser, L., Plouraboué, F., Descombes, X.: Gap filling of 3-d microvascular networks by tensor voting. *IEEE transactions on medical imaging* **27** (2008) 674–687
17. Leng, Z., Korenberg, J.R., Roysam, B., Tasdizen, T.: A rapid 2-d centerline extraction method based on tensor voting. In: *IEEE international symposium on biomedical imaging: From nano to macro*. (2011) 1000–1003
18. Medioni, G., Lee, M.S., Tang, C.K.: *A computational framework for segmentation and grouping*. Elsevier (2000)
19. Otsu, N.: A threshold selection method from gray-level histograms. *Automatica* **11** (1975) 23–27
20. Jain, A.K.: *Fundamentals of digital image processing*. Prentice-Hall, Inc. (1989)
21. Medioni, G., Tang, C.K., Lee, M.S.: Tensor voting: Theory and applications. *Proceedings of RFIA, Paris, France* **3** (2000)
22. Wu, T.P., Yeung, S.K., Jia, J., Tang, C.K., Medioni, G.: A closed-form solution to tensor voting: Theory and applications. *IEEE Trans Pattern Anal Mach Intell* **34** (2012) 1482–1495
23. Loss, L., Bebis, G., Nicolescu, M., Skurikhin, A.: An iterative multi-scale tensor voting scheme for perceptual grouping of natural shapes in cluttered backgrounds. *Computer Vision and Image Understanding* **113** (2009) 126–149
24. Deutsch, S., Medioni, G.: Intersecting manifolds: detection, segmentation, and labeling. In: *AAAI*. (2015) 3445–3452
25. Christodoulidis, A., Hurtut, T., Tahar, H.B., Cheriet, F.: A multi-scale tensor voting approach for small retinal vessel segmentation in high resolution fundus images. *Computerized Medical Imaging and Graphics* (2016)